



A Comparative Study Between Conventional Outrigger System and Hybrid Outrigger System considering Performance Index Criterion

Neethu Elizabeth John¹ · Kiran Kamath¹

Received: 23 February 2024 / Accepted: 20 June 2024 / Published online: 26 July 2024
© The Author(s) 2024

Abstract Outriggers are regarded as a structural component which can effectively lessen the reactions generated by lateral loads in tall buildings. Depending on the connectivity between the core and the peripheral columns, the outrigger system can be divided into virtual outrigger system and conventional outrigger system (COS). The hybrid outrigger system (HOS) has one conventional outrigger and one virtual outrigger at two distinct floor levels. This study gives a comparison of optimal position and performance between COS and HOS based on formulated performance index criterion (PIC) for building heights of 140, 210, 280 and 350 m by considering variations in stiffness of the outrigger belt wall and beam, the stiffness of the building's core, the height of the structure and the length of the outrigger arm under static wind and equivalent static earthquake load. The outrigger behaviour assessed using PIC takes into account the combined response of displacement at top, absolute maximum inter storey drift ratio and acceleration response at the roof. Based on PIC, performance of both COS and HOS at their evaluated optimal position are compared, and is found that HOS are less effective than COS. Therefore, to enhance the performance of HOS to be in par with COS, an optimization study is performed by increasing the axial stiffness of column, stiffness of outrigger, and stiffness of slab while maintaining the increase in total concrete volume of the structure a minimum. From the findings, PIC values

of HOS (PIC_{HOS}) for 40 to 100 storeys exhibits an increase of 10 to 1.1, 20.2 to 2.2 and 12.5 to 1.9% for variation in core thickness, length of outrigger arm, and outrigger thickness, respectively, compared to PIC values of COS (PIC_{COS}). For PIC_{HOS} to be comparable with PIC_{COS} , increase in the total concrete volume of HOS reduces from 1.4–16.5 to 0.6–2.5% as the model's height increases from 40 to 100 storeys, respectively, suggesting that the HOS with marginal increase in total concrete volume can perform effectively for taller structures.

Keywords Hybrid outrigger system · Conventional outrigger system · Performance index criterion · Parametric analysis · Comparative analysis · Optimization study

Introduction

The outrigger design principle is often used in the construction of tall buildings. The outrigger system has become increasingly relevant due to its capacity to enhance the building's behaviour performance under seismic and wind stimulation. Extending from the load-resisting core to columns on the building's facade, outrigger walls are connected. Depending on the connectivity between the core and the peripheral columns, the outrigger system can be divided into virtual outriggers and conventional outriggers. Space restriction at the level of outrigger and challenges in architectural planning is a limitation in conventional outriggers due to its direct connection between the core wall and exterior columns. Virtual outriggers were created as an option to solve these challenges; they transfer moments indirectly through floor diaphragms [1]. The vertical belt wall obtains the equivalent horizontal couple from the semi-rigid floor diaphragms and changes it into

✉ Kiran Kamath
kiran.kamath@manipal.edu
Neethu Elizabeth John
neethuejohn@gmail.com

¹ Department of Civil Engineering, Manipal Institute of Technology, Manipal Academy of Higher Education, Manipal, India

a vertical couple before transmitting it to the columns, and this movement lessens the core's bending moment [1]. Conventional Outriggers (CO) which connects the core and outer columns directly with the outrigger arms, creates compression forces and tension forces in the leeward columns and windward columns, respectively to transfer forces bringing down the core moment [2–4]. The conventional outrigger offers a superior reduction in lateral deformation compared to the virtual outrigger because conventional outriggers have the arms directly connected between the columns and the core [1, 5]. Virtual outriggers (VO) can be installed to solve space related issues created by conventional outrigger arms, allowing the floor to be occupied and increasing cost efficiency. A novel system called the hybrid outrigger system with one conventional and one virtual outrigger at two different floor levels is designed in this study, taking into account both the improved performance of conventional outriggers and the space effectiveness of virtual outriggers.

In order to lower the connection costs in complex connectivity between composite or steel outriggers and concrete core, a reinforced concrete outrigger and core are considered for the analysis in this study [6]. According to the wind and seismic loading circumstances, different structural systems has different ideal placements [7]. The position of the outriggers is seen to be affected differently by the response and stiffness parameters which is taken into account. The optimum location of the outrigger varies depending on the response parameter considered to assess the behavioural characteristics of the structural system. While varying the stiffness parameters, the outrigger response has been accounted considering values of base shear reaction, moment at the base, displacement at top, inter storey drift ratio, acceleration response at the roof, column forces, time period and frequency [8–15]. This study is based on a performance index criteria (PIC) which takes into account the combined response of displacement at top, inter storey drift ratio and acceleration response at the roof. The formulation of PIC is explained in Sect. (Procedure for analysis and evaluation of optimal position using Performance Index Criterion (PIC)). The Performance index criterion is used to assess structure's overall response than to analyse each dependent parameter separately [16–18].

A considerable amount of research on concrete outrigger systems, according to prior literature assessments, has only been done on conventional outriggers, facade riggers, virtual outriggers, outriggers with belt truss/wall, and outriggers installed with dampers. The study of conventional and virtual outriggers in a single structure, which is phrased Hybrid Outrigger System (HOS) in this research work, is understudied in the previous literature. When comparing hybrid outrigger systems to Conventional Outrigger System (COS), conventional outrigger systems efficiency would be

better; however, the behavioural performance of the HOS can be improved by altering the proportions of the structural components.

In this study, the stiffness of the outrigger belt wall and beam, the stiffness of the building's core, the structural height and the length of the outrigger arm are considered as the stiffness variables used to examine the behaviour of HOS and COS. The above-mentioned independent factors are represented by a dimensionless parameter β , taken as the relative stiffness ratio between core and outrigger. The optimal placements under static wind and equivalent static earthquake loads are calculated for a total of 12 β values, taking the PIC into account for both COS and HOS, and a comparison of optimal locations and performance based on PIC between HOS and COS is carried out. However, hybrid outriggers are less effective than conventional outriggers with the same structural component dimensions due to their reduced rigidity at the virtual outrigger floor of HOS which has an indirect force transmission mechanism. Therefore, a study on the enhancement of the performance of HOS is carried out by increasing the bending stiffness of slabs, axial stiffness of columns, and bending stiffness of outriggers by certain folds for the formulated β values keeping the increase in total concrete volume of the structure a minimum. The behavioural analysis is performed for four different heights of 140, 210, 280 and 350 m having 40, 60, 80 and 100 storeys in a finite element software, ETABS. The parametric analysis and their corresponding results are given under Sects. ('Methodology') and ('Analysis Results') respectively.

In [16], the authors have studied the static and dynamic behaviour of hybrid outrigger system based on stiffness of core, stiffness of outrigger beam and belt wall, length of the outrigger arm, and height of the building as varying parameters, and investigated on optimal positions of hybrid outrigger system under wind and earthquake loads. In [17], authors have investigated the influence of variation in the column area on hybrid outrigger system for wind and seismic loads. In [18], authors have discussed the influence of slab structure on the behavioural analysis of hybrid outrigger system.

This study is an extension work of the author's initial study on hybrid outrigger system [16]. From the results of the previous studies [16–18] it can be inferred that HOS can be utilised as an efficient lateral load resisting system. But, when comparing the performance of HOS to the COS, the COS shows an improved lateral load resistance. As the COS has direct transfer of forces, its performance in reducing the lateral loads will be better compared with HOS. Therefore, a study is required to quantify how much the COS is better compared with HOS in terms of its lateral resistance. Thus, this study quantifies and compares the efficiency of both the outrigger systems using

a performance based analysis, and also portrays how the performance of HOS can be enhanced to be comparable to COS using an optimization study.

Methodology

Parametric Definitions

The independent parameters considered for this research are stiffness of core and outrigger, outrigger arm length and structural height. These factors are varied over a specific range and the analysis is done for those variations. The independent factors stated above are consolidated to form a dimensionless factor termed β considered as the ratio of relative stiffness of core to relative stiffness of outrigger [2] and is formulated as in Eq. 1, where, E is concrete elastic modulus, I_{core} and I_o being moment of inertia of core and outrigger respectively, d being the width of the considered model and H being the total structural height.

$$\beta = \frac{EI_{core}}{EI_o} * \frac{d}{H} \tag{1}$$

The expressions to calculate the moment of inertia of core, conventional outrigger and virtual outrigger is explained in John and Kamath (2022) [16]. As the hybrid outrigger has both conventional and virtual outrigger, the moment of inertia of VO and CO are calculated separately for the formulation of the β values. By altering the width of the building d , outrigger thickness t_o , and core thickness t_{core} across a defined range, 12 values for the parametric analysis are produced. For consistency, the breadth of the core wall b is kept at 18 m for the models studied, whereas t_{core} is altered accordingly while maintaining a constant ratio of area of floor to area of core wall. The design variables shown in

Table 1 are used to calculate the values of β_{CO} and β_{VO} for the four building heights considered.

Locations Where Outriggers are Placed for the Evaluation of Optimal Positions

In order to provide for spacious foyer areas, the lowest level for the base outrigger is set for all models at the fifth story. The separation between the lower and higher outrigger is set for all models at H/3, where H is the height of the structure. A pilot study was performed for calculating the interval between CO and VO which is explained in John and Kamath, 2022 [16]. The optimal separation gap is obtained as H/3 and the analysis’s findings corroborated those found in earlier studies by Smith and Coull, 1991; Patil and Sangle, 2016; Moon, 2016; Samarakkody et al., 2017; and Che and Zhang, 2018 [2, 13, 19–21]. Table 2 lists the floor placements for the 40, 60, 80, and 100 storey models under consideration, along with their respective relative heights for both conventional and virtual outrigger.

Six placements of the hybrid outrigger are selected for models with 40 stories. The CO is below the VO in the first three sets, which are italicised (*1–40-sq*, *2–40-sq*, *3–40-sq*) but VO is below the CO in the next three sets, bolded (**4–40-sq**, **5–40-sq**, **6–40-sq**). Similarly, in 60, 80, and 100 storey models, hybrid outriggers contain 8, 10, and 14 locations, respectively, with the first 4 locations in 60, 5 in 80, and 7 in 100 storey models representing CO below VO (italicised) and the remaining locations for VO below CO (bolded). In conventional outrigger model the same position is adopted replacing virtual outrigger with another conventional outrigger. Therefore, the positions marked in bold are not applicable for conventional outrigger models. The outrigger positions are varied along the height of the building placing the outriggers at the positions mentioned in Table 2 and the optimal positions based on PIC is evaluated for the formulated β values in Table 1.

Table 1 Variables (assumed values) for β_{CO} and β_{VO} used in practical design [16]

Sl. no	t_{core} (mm)	d (m)	t_o (mm)	β values for the studied models							
				β_{CO-40}	β_{VO-40}	β_{CO-60}	β_{VO-60}	β_{CO-80}	β_{VO-80}	β_{CO-100}	β_{VO-100}
1	405	35	800	137.79	7.35	91.9	4.9	68.9	3.7	55.1	2.9
2	535	35	800	182.09	9.71	121.4	6.5	91.0	4.9	72.8	3.9
3	680	35	800	231.57	12.35	154.4	8.2	115.8	6.2	92.6	4.9
4	850	35	800	289.69	15.45	193.1	10.3	144.8	7.7	115.9	6.2
5	405	35	650	169.59	7.35	113.1	4.9	84.8	3.7	67.8	2.9
6	405	40	650	193.82	7.35	129.2	4.9	96.9	3.7	77.5	2.9
7	405	45	650	218.05	7.35	145.4	4.9	109.0	3.7	87.2	2.9
8	405	50	650	242.27	7.35	161.5	4.9	121.1	3.7	96.9	2.9
9	535	40	500	332.97	9.71	222.0	6.5	166.5	4.9	133.2	3.9
10	535	40	650	256.13	9.71	170.8	6.5	128.1	4.9	102.5	3.9
11	535	40	800	208.11	9.71	138.7	6.5	104.1	4.9	83.2	3.9
12	535	40	950	175.25	9.71	116.8	6.5	87.6	4.9	70.1	3.9

Table 2 Relative outrigger positions for 40, 60, 80 and 100 storey models [18]

Number of storey's	Interval between outrigger	Abbreviation	CO floor location	VO floor location	CO relative location	VO relative location
40	13	<i>1-40-sq</i>	5	18	0.125	0.450
		<i>2-40-sq</i>	15	28	0.375	0.700
		<i>3-40-sq</i>	25	38	0.625	0.950
		4-40-sq	18	5	0.450	0.125
		5-40-sq	28	15	0.700	0.375
		6-40-sq	38	25	0.950	0.625
60	20	<i>1-60-sq</i>	5	25	0.083	0.417
		<i>2-60-sq</i>	15	35	0.250	0.583
		<i>3-60-sq</i>	25	45	0.417	0.750
		<i>4-60-sq</i>	35	55	0.583	0.917
		5-60-sq	25	5	0.417	0.083
		6-60-sq	35	15	0.583	0.250
		7-60-sq	45	25	0.750	0.417
		8-60-sq	55	35	0.917	0.583
80	27	<i>1-80-sq</i>	5	32	0.063	0.400
		<i>2-80-sq</i>	15	42	0.188	0.525
		<i>3-80-sq</i>	25	52	0.313	0.650
		<i>4-80-sq</i>	35	62	0.438	0.775
		<i>5-80-sq</i>	45	72	0.563	0.900
		6-80-sq	32	5	0.400	0.063
		7-80-sq	42	15	0.525	0.188
		8-80-sq	52	25	0.650	0.313
		9-80-sq	62	35	0.775	0.438
		10-80-sq	72	45	0.900	0.563
100	33	<i>1-100-sq</i>	5	38	0.05	0.38
		<i>2-100-sq</i>	15	48	0.15	0.48
		<i>3-100-sq</i>	25	58	0.25	0.58
		<i>4-100-sq</i>	35	68	0.35	0.68
		<i>5-100-sq</i>	45	78	0.45	0.78
		<i>6-100-sq</i>	55	88	0.55	0.88
		<i>7-100-sq</i>	65	98	0.65	0.98
		8-100-sq	38	5	0.38	0.05
		9-100-sq	48	15	0.48	0.15
		10-100-sq	58	25	0.58	0.25
		11-100-sq	68	35	0.68	0.35
		12-100-sq	78	45	0.78	0.45
		13-100-sq	88	55	0.88	0.55
		14-100-sq	98	65	0.98	0.65

Modelling Details and Loading Conditions

The benchmark model has a core wall that is 18 m wide and no outriggers placed. Figure 1a shows the floor plan at CO level of $\beta_{CO-40} = 332.97$ and respective $\beta_{VO-40} = 9.71$. Figure 1b and c shows the 3-D view for HOS and COS model. The length of outrigger arm is represented by l_o , and for 35 m wide models it is 8.5 m and is incremented from 8.5 to 16 m in 2.5 m increment varying the width of the model from 35 to 50 m in the models considered for this study.

Along both x and y axis, the models are symmetrical and are analysed in a finite element software, ETABS. The individual storey height is assumed to be 3.5 m and the compressive strength of concrete is taken as 60 MPa. The loads are defined as per IS codes. The models are subjected to static wind and earthquake loads (EQ). Slab thickness at outrigger level is taken as 250 mm to carry the higher loads of outriggers [22–24] and other floors has a typical slab thickness of 180 mm.

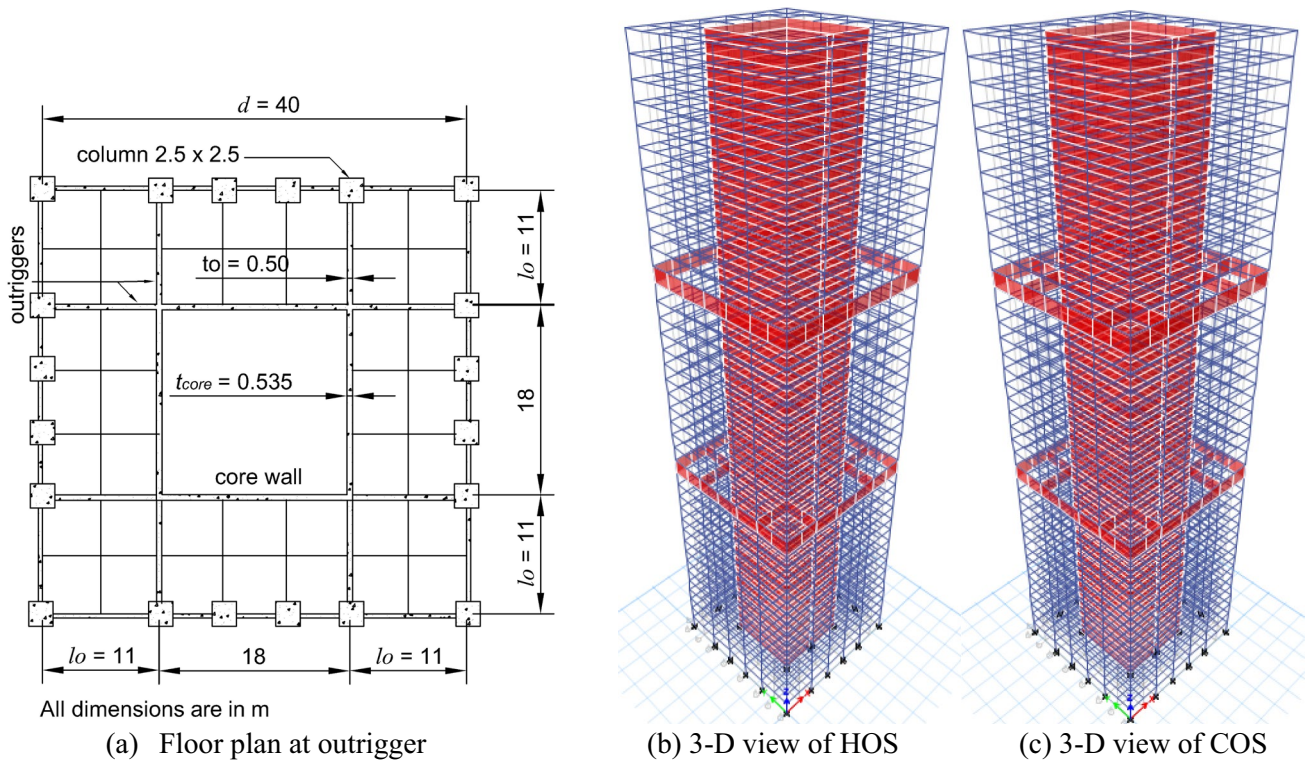


Fig. 1 Plan at the floor level of outrigger and 3-D view for conventional and hybrid outrigger system

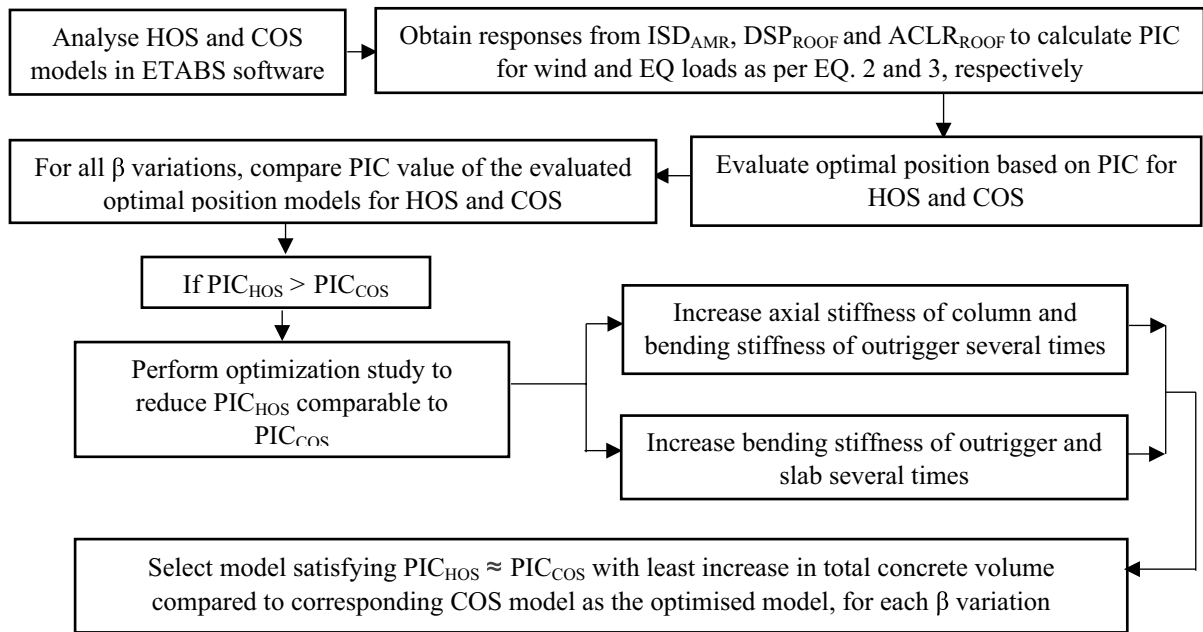


Fig. 2 Flow chart showing optimization procedure used in the investigation

The slabs are given a super dead load of 1.5 kN/m², a live load of 3.5 kN/m², and a live load of 1.5 kN/m² on the roof [25, 26]. The IS codes [27, 28] are utilised to calculate the

wind speed, pressure coefficients, and seismic zone factor on the assumption that the structure is located in Mumbai. The seismic zone and wind speed are 0.16—III and 44 m/s,

respectively. Shell-thin modelling is used to design the outriggers and core wall as wall sections. Frame elements is used to represent beams and columns and shell-thin elements are defined for slabs. Semi-rigid diaphragms are defined to the slabs linking the outrigger walls in order to simulate real in-plane stiffness characteristics and the transmission of force through beams and slabs attached to the VO walls. Static wind and equivalent static earthquake analysis are performed on all models in accordance with IS standards.

Procedure for Analysis and Evaluation of Optimal Position Using Performance Index Criterion (PIC)

In this research work, both the considered outrigger system’s behaviour is analysed using a set of parameters, and from the analysis findings, the system’s optimum location is determined. The core stiffness, stiffness of outrigger belt wall and beam, the width of the building are varied within a certain range as in Table 1 and those are formulated to give a dimensionless parameter termed β . For these β variations, the hybrid and conventional outrigger system structures are modelled. Four different heights are considered for the comparison. Heights of 140, 210, 280 and 350 m having 40, 60, 80 and 100 storeys are considered for the analysis. The location of the outriggers are varied along the structure height as per the floor positions mentioned in Table 2 for each β variation. A total of 684 models are analysed using ETABS software. The modelling details and loading conditions are given in Sect. (‘Modelling

details and loading conditions’). The models are analysed for static wind and equivalent static earthquake loads. The behaviour of hybrid and conventional outrigger system is assessed based on the responses from absolute maximum inter storey drift ratio (ISD_{AMR}), displacement at the roof (DSP_{ROOF}) and acceleration at the roof ($ACLR_{ROOF}$). The $ACLR_{ROOF}$ is calculated for the wind loads alone using IS 875-3-2015 [27]. Once the responses from the above dependent parameters are obtained, the optimal position for both hybrid and conventional outrigger system based on PIC is evaluated.

John and Kamath, 2022 [16] outline the steps involved in determining the ideal location based on PIC. Equations 2 and 3, respectively, provide the equations for calculating the performance index for wind and EQ loads.

$$PIC_{wind} = \frac{ISD_{AMR}}{ISD_{AMR\ limit}} + \frac{DSP_{ROOF}}{DSP_{ROOF\ limit}} + \frac{ACLR_{ROOF}}{ACLR_{ROOF\ limit}} \tag{2}$$

$$PIC_{EQ} = \frac{ISD_{AMR}}{ISD_{AMR\ limit}} + \frac{DSP_{ROOF}}{DSP_{ROOF\ limit}} \tag{3}$$

The limit values for DSP_{ROOF} , $ACLR_{ROOF}$, and ISD_{AMR} are determined using codes IS 16700 [29] and IS 456 [30], and are taken to be $H/500$, 250 mm/s^2 , and $1/400$, respectively for wind loading, and $H/500$ for DSP_{ROOF} [31, 32] and $1/250$ for ISD_{AMR} [29] for EQ loads. The results of the analysis performed for each model under each load and outrigger position serve as the numerator values. Equations 2 and 3

Table 3 Percentage reduction values under wind loads in 40 storey models for β values considered in studying the increase in outrigger thickness

COS	HOS		Dependent parameters	Outrigger positions of HOS						Outrigger positions of COS		
	β_{CO-40}	β_{VO-40}		1-40-sq	2-40-sq	3-40-sq	4-40-sq	5-40-sq	6-40-sq	1-40-sq	2-40-sq	3-40-sq
332.97	332.97	9.71	ISD_{AMR}	20.05	32.97	39.46	42.1	29.19	27.03	44.32	50.81	41.08
			DSP_{ROOF}	33.8	42.98	42.5	42.67	43.06	37.41	46.44	51.18	45.96
			$ACLR_{ROOF}$	27.18	33.94	35.55	33.00	35.44	33.89	35.12	40.15	39.33
			BM_{base}	44.12	36.87	29.37	37.75	30.39	25.80	50.44	38.94	30.14
256.13	256.13	9.71	ISD_{AMR}	21.08	34.59	40.54	43.78	29.73	27.57	45.41	51.89	41.62
			DSP_{ROOF}	34.53	44.04	43.49	43.91	44.06	37.99	47.82	52.43	46.84
			$ACLR_{ROOF}$	27.80	34.70	37.27	33.75	36.25	34.71	35.93	41.22	40.34
			BM_{base}	45.96	37.81	29.83	38.68	30.83	26.00	52.18	39.83	30.55
208.11	208.11	9.71	ISD_{AMR}	21.62	35.68	41.08	44.86	30.27	28.11	46.49	52.97	42.16
			DSP_{ROOF}	35.12	34.83	44.24	44.81	44.84	38.43	48.87	53.37	47.50
			$ACLR_{ROOF}$	28.04	35.35	37.94	34.36	36.96	35.56	36.71	42.06	41.25
			BM_{base}	42.10	32.76	23.82	33.69	24.88	20.50	48.81	34.87	44.55
175.25	175.25	9.71	ISD_{AMR}	21.62	36.22	41.62	45.11	30.81	28.65	47.03	54.05	42.70
			DSP_{ROOF}	35.61	45.34	44.85	45.35	45.46	38.78	49.72	54.12	48.02
			$ACLR_{ROOF}$	28.37	35.81	38.10	34.94	37.68	36.70	37.24	42.82	42.01
			BM_{base}	48.34	39.13	30.47	39.99	31.45	32.90	54.61	41.05	31.12

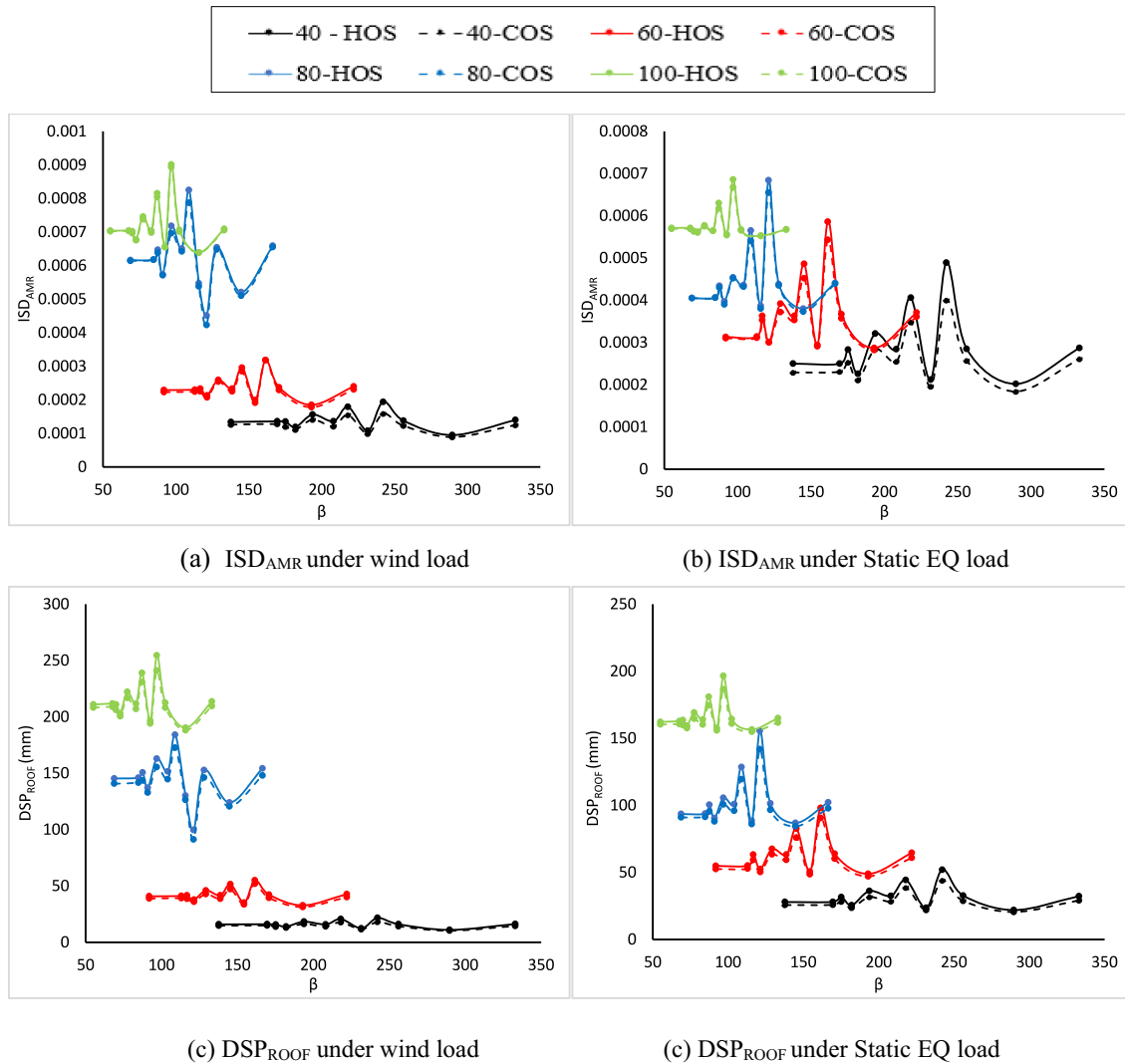


Fig. 3 Comparison between conventional and hybrid outrigger system in terms of ISD_{AMR} and DSP_{roof} at their optimal position for 40, 60, 80 and 100 storey models

are then used to compute the PIC values for each model. Acceleration is one of the dominant factors in tall buildings which can affect the human sensation to vibrational motion. The acceleration effect is considered in the PIC calculation for wind loads (Eq. 2) as their occurrence is very frequent, but not in the case of earthquakes (Eq. 3), as they are non-frequent. From the results, the models with outriggers had lower values and the control or benchmark model has the highest PIC value. Therefore, from the various outrigger positions for each β variation, the location with the lowest PIC value is chosen as the optimal location. This is done for each β variation under each load for 40, 60, 80, and 100 storey for both hybrid and conventional outrigger models.

Performance investigation based on PIC between HOS and COS is conducted once the optimum position determined by PIC had been identified. To improve the

performance of hybrid outrigger system, an optimization study with minimal increase in total concrete volume of the structure has been conducted where the PIC for HOS (PIC_{HOS}) has been reduced to the PIC for COS (PIC_{COS}) by increasing the stiffness of independent parameters. For investigating the performance between HOS and COS, the performance index values, PIC_{wind} and PIC_{EQ} for the obtained optimal position model based on PIC are compared. For instance, taking a particular β value, the PIC_{wind} at the optimal position obtained for HOS is compared to the PIC_{wind} for COS at its optimal position. The better performance would be portrayed by the one with lower PIC values. This is done for both wind and EQ loads. The models with HOS at their optimal position has a higher PIC_{wind} and PIC_{EQ} value compared to the COS at its optimal position. Therefore, to enhance the performance of HOS, the axial

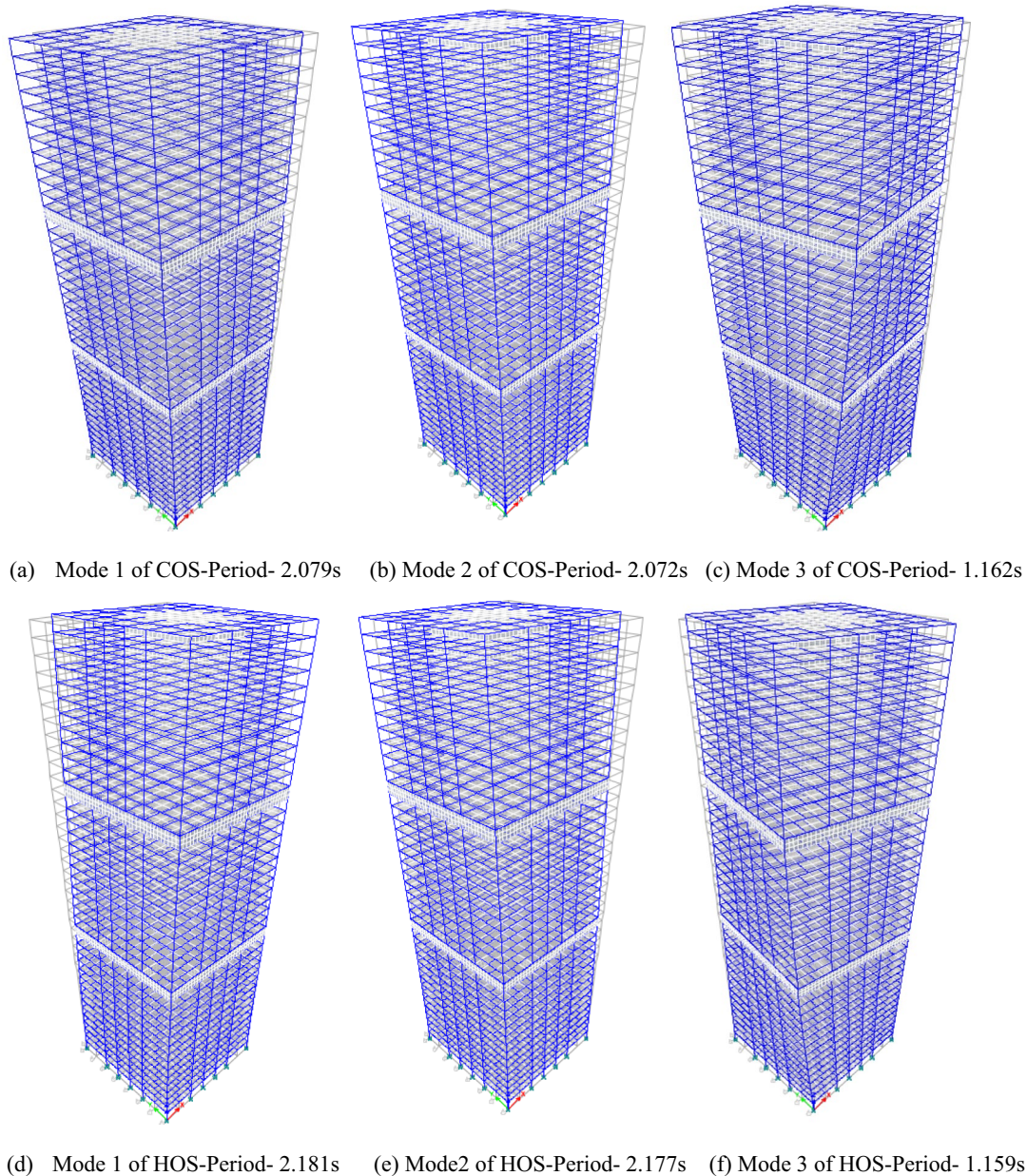


Fig. 4 Mode shapes and corresponding time period of building with COS and HOS for $\beta_{co} = 40 = 175.25$

stiffness of column, bending stiffness of outrigger beam and slab are varied to bring down the PIC values of HOS comparable or lesser than the values of COS under both wind and EQ loads. This is performed for all four building heights.

Various trial models are analysed by increasing the stiffness parameters for the PIC_{HOS} to be in par with PIC_{COS} and the one which gives the least increase in total concrete volume is taken as the optimized model. The percentage increase in total concrete volume of the structure and increase in stiffness parameters are accounted for the comparison study. The results of optimal position based on PIC and comparison between HOS and COS is given under Sect.

(‘Analysis Results’). Figure 2 provide a flow chart for better clarification of the procedure followed for the optimization study used in this investigation.

Analysis Results

Performance Comparison Between Hybrid Outrigger System and Conventional Outrigger System

To analyse the efficiency of hybrid outrigger system over conventional outrigger system, the percentage reduction in

Table 4 Sample representation of PIC_{wind} for $\beta_{CO} - 60 = 91.9$ and $\beta_{VO} - 60 = 4.9$

Outrigger location	ISD_{AMR}	DSP_{ROOF} (mm)	$ACLR_{ROOF}$ (mm/s^2)	PIC_{wind}
<i>Hybrid outrigger system</i>				
CONTROL	0.000261	45.89	84.72	0.553
1-60-sq	0.000245	42.16	81.61	0.525
2-60-sq	0.000237	40.60	80.10	0.512
3-60-sq	0.000227	40.78	79.84	0.507
4-60-sq	0.000244	41.90	79.55	0.516
5-60-sq	0.000229	40.58	80.37	0.510
6-60-sq	0.000237	40.82	79.93	0.512
7-60-sq	0.000242	41.97	79.99	0.517
8-60-sq	0.000254	43.40	80.45	0.527
<i>Conventional outrigger system</i>				
1-60-sq	0.000229	39.75	79.89	0.506
2-60-sq	0.000225	38.88	78.72	0.497
3-60-sq	0.000223	39.77	78.47	0.498
4-60-sq	0.000245	41.55	78.88	0.512

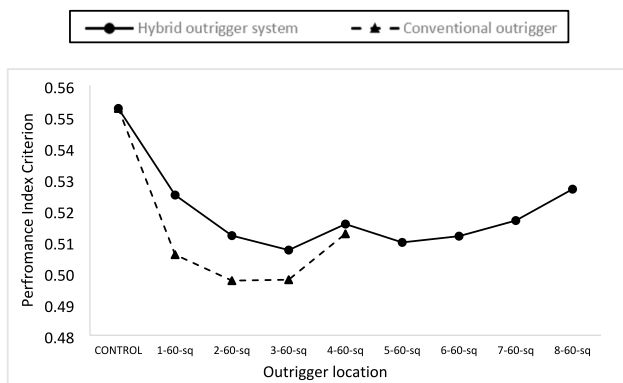


Fig. 5 Representation of variation in PIC for various outrigger positions in HOS and COS for the PIC_{wind} values in Table 4

the values of ISD_{AMR} , DSP_{ROOF} and $ACLR_{ROOF}$ are compared for both systems placed at the same floor level keeping the bench mark model as the model with core wall alone. For instance, Table 3 shows a comparison of percentage reduction in the dependent parameters for β values formulated for increase in outrigger thickness under wind loads for 40 storey models under various outrigger positions as in Table 2.

The benchmark model considered is model with core wall alone and the response of the HOS and COS is compared to the benchmark model response so as to calculate the percentage reduction values. The values marked in bold shows the maximum reduction in the responses for both COS and HOS, and is visible that the COS offers a better performance when compared to HOS models. Base bending moment (BM_{BASE}) is also compared in Table 3. Similar performance pattern is

noticed for other heights as well. Comparing all the building heights, the optimal position evaluated for conventional outrigger system is nearly obtained at 1/3rd and 2/3rd position of the building height and is close to the optimal locations obtained for COS from the previous research studies [2, 13, 19–21]. It is also noticed that the performance of COS is slightly better than the HOS because of the increased stiffness of conventional outrigger arms.

Figure 3 gives a comparison between conventional and hybrid outrigger system in terms of ISD_{AMR} and DSP_{ROOF} at their optimal position under wind and earthquake loads for 40, 60, 80 and 100 storey models. On comparing the results of HOS to COS from 40 to 100 storeys, the percentage increase in the values of ISD_{AMR} , DSP_{ROOF} and $ACLR_{ROOF}$ for HOS are within 12.5–1% for t_{core} and t_o variations, but a percentage increase of 22–1% is observed for l_o variations. This is because of the increased relative stiffness of core to outrigger and reduced aspect ratio. But, incorporating hybrid outrigger system can make the structure more economical as the virtual outrigger can eliminate the problem of space obstruction due to outrigger arms, thus utilizing that floor for occupants. Once the responses from the above dependent parameters are obtained for all the building heights, the optimal position for both hybrid and conventional outrigger system based on PIC is evaluated.

The mode shapes of the models with COS and HOS have been studied. The natural period of fundamental torsional mode of vibration is not exceeding 0.9 times the smaller of the natural periods of the fundamental translational modes of vibration in each of the orthogonal directions in any of the cases. The Fig. 4 gives sample representation of the first three mode shapes of COS and HOS for $\beta_{CO} - 40 = 175.25$ having position at 2–40-sq. Similarly, for other models, vibration in mode 3 is not exceeding 0.9 times smaller of natural periods in orthogonal directions (mode 1 and 2).

Optimal Positions of Hybrid Outrigger System Using Performance Index Criterion (PIC)

The response values of the dependent parameters ISD_{AMR} , DSP_{ROOF} and $ACLR_{ROOF}$ is computed for both COS and HOS under both wind loads and equivalent static earthquake loads in 40, 60, 80 and 100 storey models. Once the response values are computed, the PIC for wind and EQ loads are calculated using the Eqs. 2 and 3. Table 4 gives a sample representation of PIC_{wind} in both HOS and COS for $\beta_{CO} - 60 = 91.9$ and $\beta_{VO} - 60 = 4.9$. From the PIC values, the one which is giving the least PIC is taken as the optimal value and the position corresponding to that is regarded as the optimal location of the outrigger for that particular β value. The optimal location based on PIC_{wind} for the structural systems compared are marked in bold under Table 4 for reference. Figure 5 gives a representation of the variation in

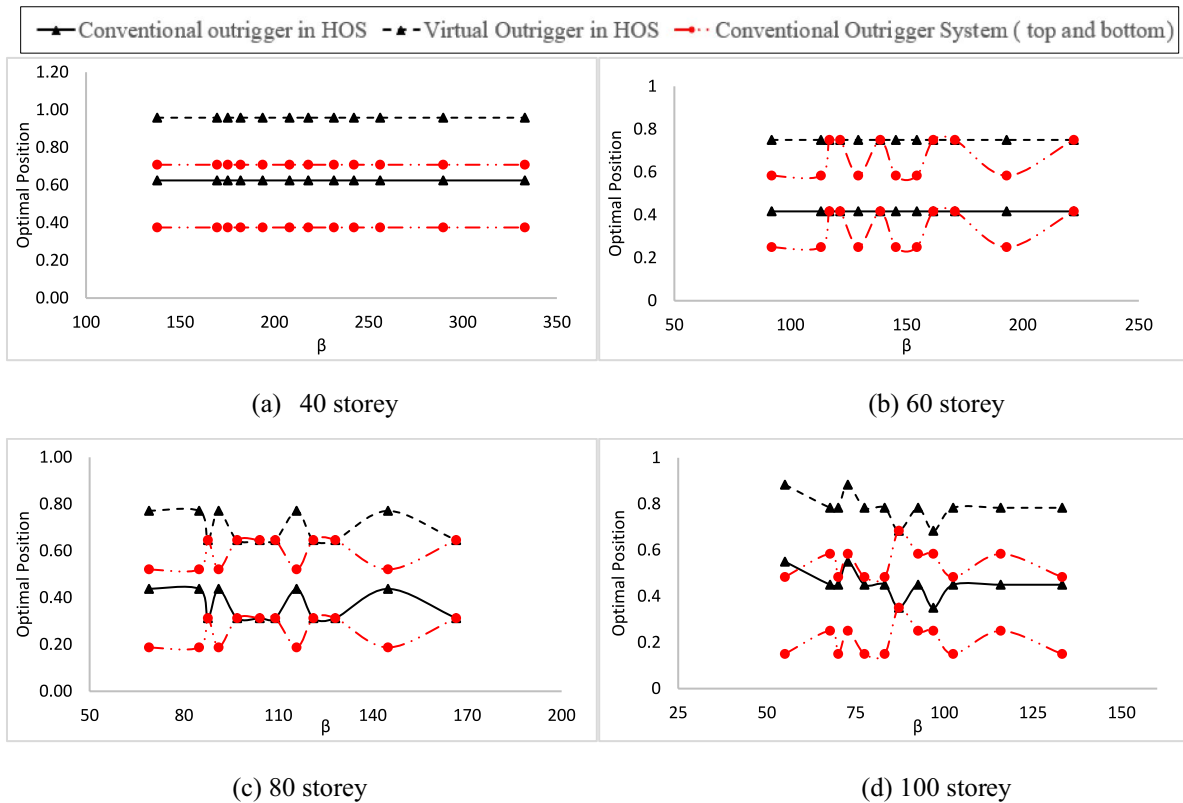


Fig. 6 Comparison of optimal location based on PIC_{wind} in both COS and HOS for 40, 60, 80 and 100 storey models

PIC for various outrigger positions in HOS and COS for the PIC_{wind} values in Table 4.

From the Fig. 5, it's visible that the PIC for HOS is greater than the values of COS which infers that, the performance of conventional outrigger system is better than the hybrid outrigger system. Even for other β values and building heights, the PIC for HOS is higher than the COS under both wind and EQ loads because of the increased stiffness offered by conventional outrigger system. After computing the optimum location of COS and HOS based on PIC for all the building heights, comparison of HOS and COS is performed. Figures 6 and 7 gives the optimal location of both the outrigger under wind and earthquake loads respectively, for all the four building heights. From Fig. 6, it's visible that the HOS has a higher optimal location than the COS for all the four building heights and the VO above the CO in HOS gives a better performance for reducing the deformations against wind loads because higher mass of CO at the top in HOS can lead to larger deformation of the structure.

From Fig. 7, which represents the optimal location under EQ loads, the COS system has a higher optimal position than the HOS in 60, 80 and 100 storey models and HOS above COS in 40 storey models. Once the optimal location based on PIC is evaluated, the PIC value for each β value at their

corresponding optimal location is compared for both HOS and COS.

From the model results, the PIC values of HOS is higher than that of COS, and for a comparison the percentage increase in PIC between both the outriggers are analysed. Figure 8a and b shows the percentage increase in the values of PIC under wind and EQ loads respectively. The rise in PIC is significantly greater for higher l_o models since the stiffness of COS increases considerably with the increase in l_o and is discernible for both the loads considered. The percentage rise in PIC is almost stagnant with increase in thickness of outrigger and diminishes slightly with rise in thickness of core under both loads considered for the study. Therefore, there is a need to improve the performance of HOS to make it comparable to the behavioural performance of COS.

Optimization Study for Improving HOS Performance in Comparison to COS

To improve the performance of hybrid outrigger system, an optimization study with minimal increase in concrete volume has been conducted where the PIC of HOS (PIC_{HOS}) has been reduced to the PIC of COS (PIC_{COS}) by increasing the stiffness of column, outrigger and slab in HOS. Maximum

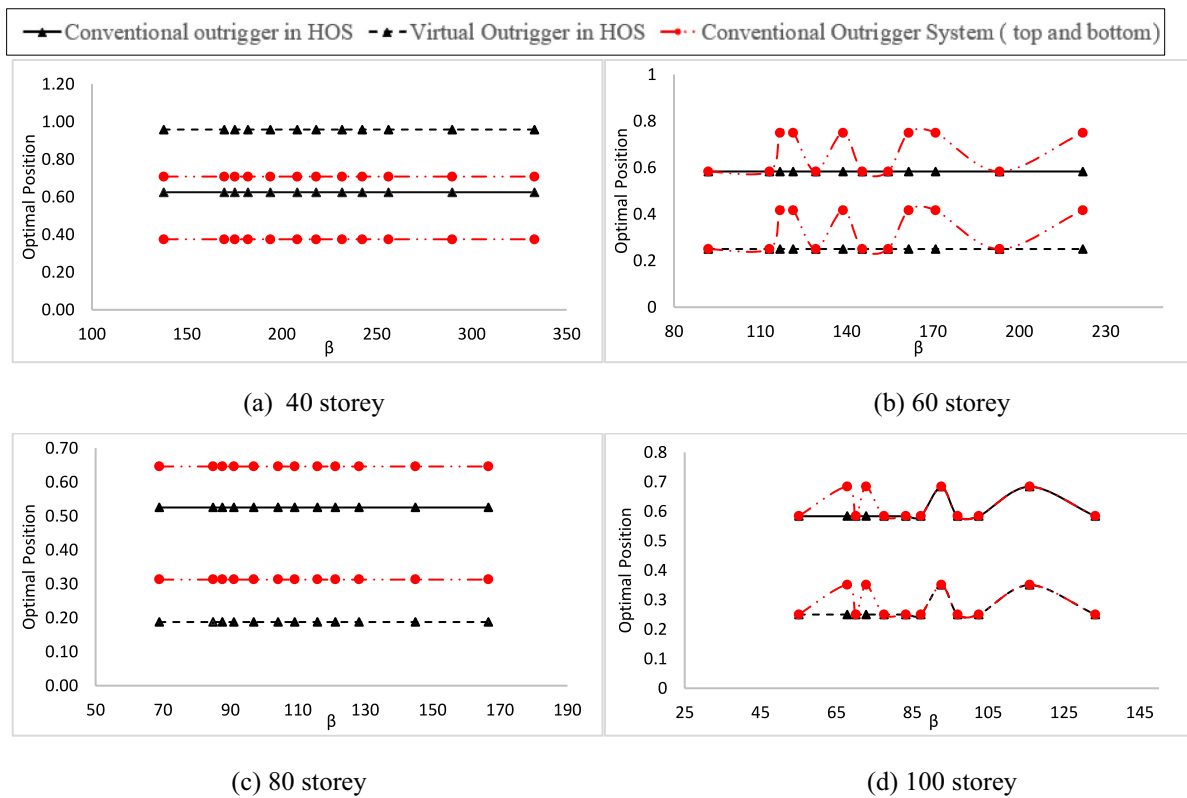


Fig. 7 Comparison of optimal location based on PIC_{EQ} in both COS and HOS for 40, 60, 80 and 100 storey models

performance or resistance of the lateral deformation happens when the outrigger is placed at its optimal position.

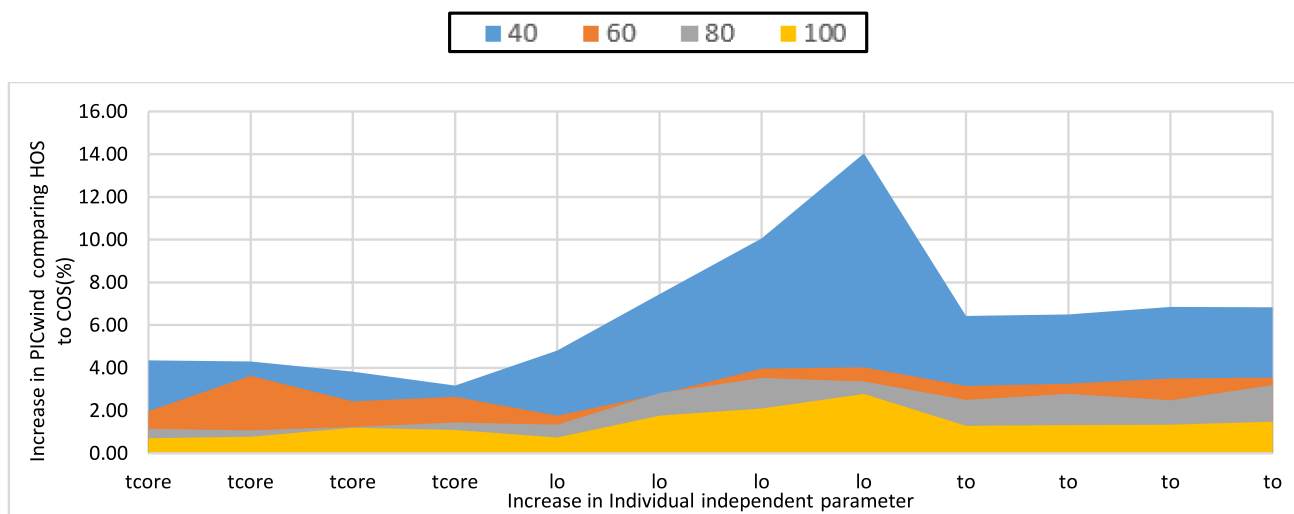
Therefore, the PIC values corresponding to HOS and COS at their optimal position have been taken for the comparative study. The study has taken four different heights of 140, 210, 280 and 350 m. For each β value considered as per Table 1, the PIC_{COS} and PIC_{HOS} have been compared, and the PIC_{HOS} has been reduced to the PIC_{COS} by increasing the stiffness of the system. This is performed for both wind and EQ load. Table 5 shows a sample calculation of the PIC values for $\beta_{CO} = 169.59$ and corresponding $\beta_{VO} = 7.35$ (40 storey model) at their optimal position. The values of independent parameters of COS for $\beta_{CO} - 40 = 169.59$ and $\beta_{VO} - 40 = 7.35$ under wind and EQ loads are shown, and for the same model parameters hybrid outrigger system has been modelled and the response at its optimal position evaluated is marked in italics in Table 5.

The stiffness of independent parameters in HOS has been modified several times to get one with least increase in concrete volume having a comparable PIC value with COS under both the loads. From Table 5, under wind loads, it's noticeable that the total increase in concrete volume is 2.59% for increase in axial stiffness in column and bending stiffness of outrigger, and is 6.8% for increase in only bending stiffness of outrigger and slab. The total increase in concrete

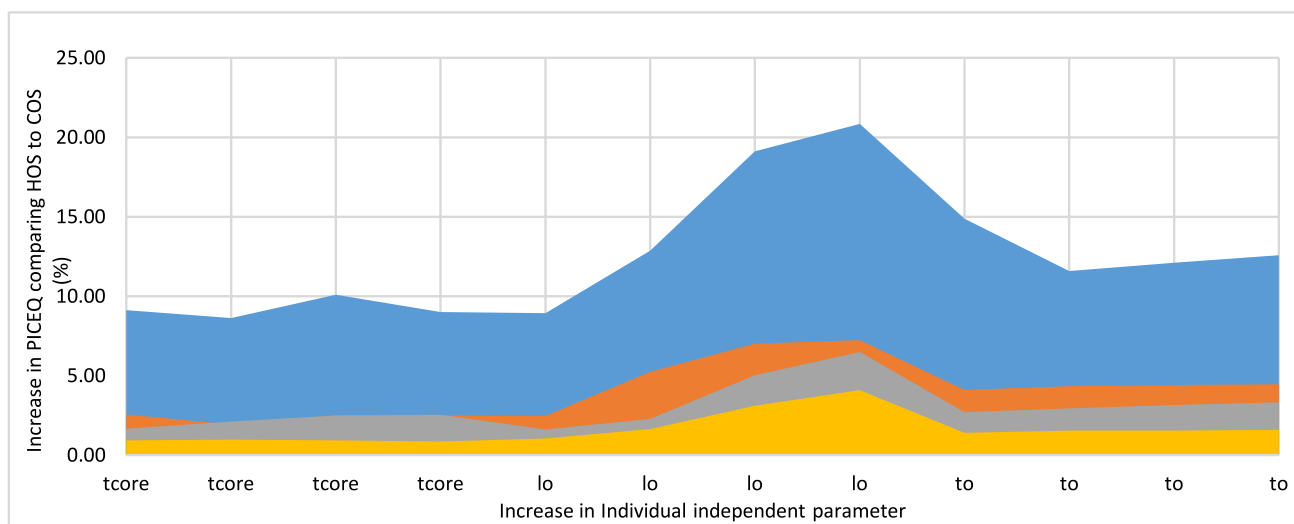
volume is observed to be higher when bending stiffness of outrigger and slab is enhanced keeping the axial stiffness of column unvaried. This effect is visible for other analysed models as well.

Under EQ loads, the PIC_{HOS} can be reduced only with increase in axial stiffness in column and a moderate increase in bending stiffness of outrigger. An increase in stiffness of slab and outrigger alone led to increase in the total seismic weight which couldn't reduce the PIC_{HOS} values effectively. A parameter termed Stiffness Magnification Factor (SMF) is used to quantify the increase in stiffness parameters considered in this optimization study. SMF has been calculated by taking the ratio of each stiffness parameter in the optimized HOS model to the respective stiffness parameter of the base COS model. For instance, in Table 5 (column-5), 1370 mm × 1370 mm is the dimension of the column in the optimized model and 1250 mm × 1250 mm is for the base COS model. The ratio of the axial stiffness between these two column dimensions is obtained as 1.1, which is termed as SMF of 1.1 for column axial stiffness.

From Table 5, it's noticeable that the PIC_{wind} has been reduced from 0.3840 to 0.3633 with a SMF of 1.1 for column axial stiffness and SMF of 1.08 for outrigger bending stiffness, and PIC_{wind} has been reduced from 0.3840 to 0.3628 with a SMF of 3.08 for outrigger bending stiffness



(a) Percentage increase in the values of PIC_{wind} when comparing HOS to COS under wind loads



(b) Percentage increase in the values of PIC_{EQ} when comparing HOS to COS under EQ loads

Fig. 8 Percentage increase in the values of PIC when comparing HOS to COS under wind and EQ loads

and SMF of 1.4 for slab stiffness. Increasing the axial stiffness of column and stiffness of outrigger alone led to a lesser value of total concrete volume increase compared to outrigger and slab stiffness increase. The PIC_{EQ} is seen to reduce from 0.1645 to 0.1505 with a SMF of 1.18 for column axial stiffness and 1.08 for outrigger bending stiffness in Table 5. Similarly for other β values, an optimization study has been conducted to make the PIC values for both COS and HOS comparable. Several times increase in the stiffness of column, outrigger and slab has been performed and the one with least increase in total concrete volume having a comparable PIC value with COS is evaluated as the optimized model under both wind and EQ loads.

Figure 9a gives a pictorial representation of the percentage increase in total concrete volume of the structure under wind loads on increasing the axial stiffness of column and outrigger stiffness alone. Figure 9b gives a pictorial representation of the percentage increase in total concrete volume of the structure under wind loads on increasing the outrigger and slab stiffness alone. Figure 9c shows the percentage increase in total concrete volume of the structure for various β values when only the column and outrigger stiffness are increased under EQ loads.

From Fig. 9, it can be noticed that with increase in height of the model, the percentage increase in concrete volume decreases except in few models of 60 and 80 storey. For

Table 5 Sample calculation of the PIC values for $\beta_{CO} - 40 = 169.59$ and corresponding $\beta_{VO} - 40 = 7.35$ (40 storey model) at their optimal position

$\beta_{CO} - 40 = 169.59$ and $\beta_{VO} - 40 = 7.35$	Conventional outrigger		Hybrid outrigger				
	Wind load	EQ load	Wind load		EQ load		
Independent parameters	*	*	*↑	*↑	*	*	*↑
Column size (mm)	1250*1250	1250*1250	1250*1250	1370*1370	1250*1250	1250*1250	1470*1470
Slab thickness (mm)	180	180	180	180	180	180	180
Core wall thickness (mm)	405	405	405	405	405	405	405
Outrigger thickness (mm)	650	650	650	700↑	2000↑	650	700↑
Mechanical slab thickness (mm)	250	250	250	250	350↑	250	250
Dependent parameters							
Displacement at top, DSP_{ROOF} (mm)	14.9	23.6	16.49	15.36	15.92	28.131	14.16
Absolute maximum Inter storey drift ratio, ISD_{AMR}	0.000128	0.000211	0.000145	0.000137	0.000141	0.000256	0.000119
Acceleration at top, $ACLR_{ROOF}$ (mm/s ²)	64.81	–	66.85	63.41	62.208	–	62.62
PIC_{wind}	0.3630	–	0.3840	0.3633	0.3628	–	–
PIC_{EQ}	–	0.1500	–	–	–	0.1645	0.1505
Volume increase in HOS model compared to COS (%)			– 0.43	2.59	6.80	– 0.43	5.26

*—Original model parameters
 *↑—Improved model parameters

40-storey models which studies the behaviour of outrigger when core thickness t_{core} is incremented, the total volume of concrete increase varied from 2.63 to 1.4% under wind loads when column and outrigger stiffness is increased (Fig. 9a), from 7.33 to 3.19% when only the outrigger and slab stiffness is increased under wind loads (Fig. 9b), and 5.91 to 3.93% only the column and outrigger stiffness is increased under EQ loads (Fig. 9c). For 100-storey models which studies the behaviour of outrigger when core thickness t_{core} is incremented, the total volume of concrete increase varied from 0.5 to 0.59% under wind loads when column and outrigger stiffness is increased (Fig. 9a), from 1.24 to 1.3% when only the outrigger and slab stiffness is increased under wind loads (Fig. 9b), and 0.77 to 0.72% only the column and outrigger stiffness is increased under EQ loads (Fig. 9c).

Comparing the aforementioned percentage values, it's noticeable that the 100-storey models has a lower % value for total volume of concrete increase. This pattern is also visible for other models which study the behaviour of outrigger when the length and thickness of the outrigger is increased. This infers that the hybrid outrigger system's ability to resist the lateral deformation is improving for taller structures when compared with COS.

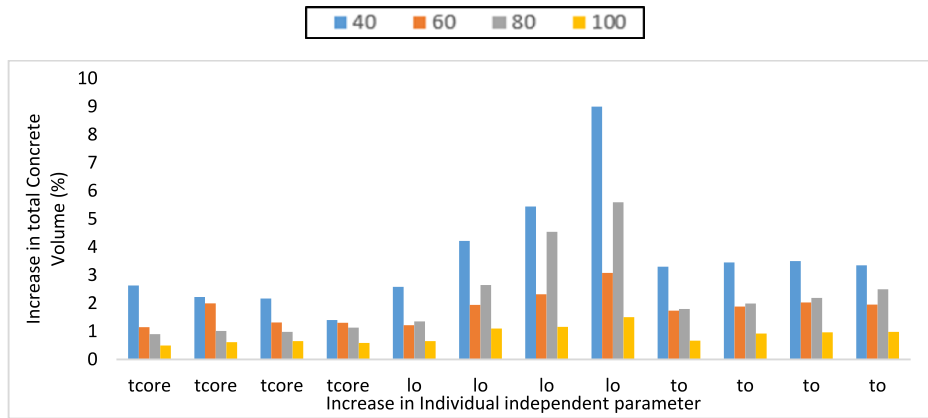
Considering all the building heights under both loads, when the length of the outrigger arm l_o is increased, the COS showed a better performance due to increased stiffness of the outrigger arm when compared with models with t_{core} and t_o increase. Therefore, for the performance of HOS to be comparable with COS, higher stiffness parameters need to be

addressed and so the increase in total volume of concrete is rising when the l_o is increased. Under wind loads, comparing Fig. 9a and b, it's noticed that the increase in concrete volume has higher values for models with outrigger and slab stiffness alone increased (Fig. 9 (b)) than for models with only the column stiffness and outrigger stiffness increased (Fig. 9 (a)). This infers that the increase in axial stiffness of column and bending stiffness of outrigger gives an effective performance for hybrid outrigger system.

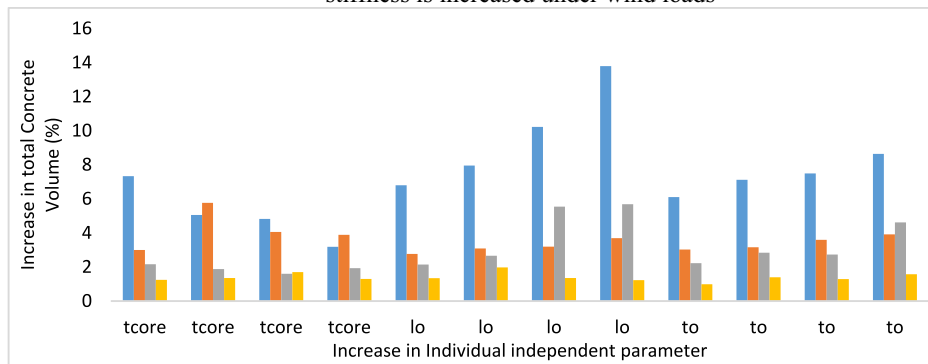
In the case of EQ loads, without increasing the axial column stiffness, the PIC_{EQ} of hybrid outrigger system isn't effectively reducing to the PIC_{EQ} of COS, so the graph between percentage increase in total concrete volume for increase in outrigger and slab stiffness alone is not portrayed. For models which study the behaviour of outrigger for increase in t_{core} and t_o , it is found that when t_{core} and t_o is increased, the increase in total concrete volume is not giving a significant variation while considering a particular height, but when the height of the model is increased from 40 to 100 storeys in 20 storey increment, a significant variation is obtained which can be noticed from the Fig. 9a, b, c.

Figure 9 illustrates the minimum increase in total concrete volume for the HOS performance to be on par with the COS performance under both wind and EQ loads while, Figs. 10, 11 and 12, demonstrate the increase in individual stiffness parameter for the same. The x-axis shows the variation of t_{core} , l_o and t_o , while the y-axis displays the variation in column, outrigger, or slab stiffness in terms of SMF.

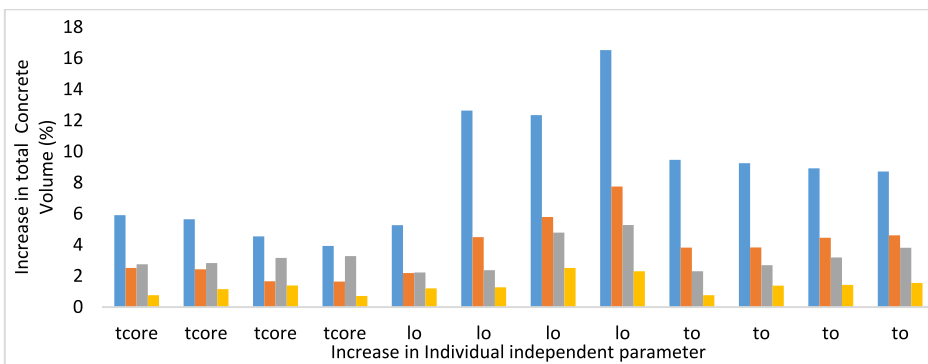
Figure 10a displays the SMF obtained for column stiffness and Fig. 10b for outrigger stiffness to optimize the HOS



(a) Percentage increase in total concrete volume of the structure when only the column and outrigger stiffness is increased under wind loads



(a) Percentage increase in total concrete volume of the structure when only the outrigger and slab stiffness are increased under wind loads



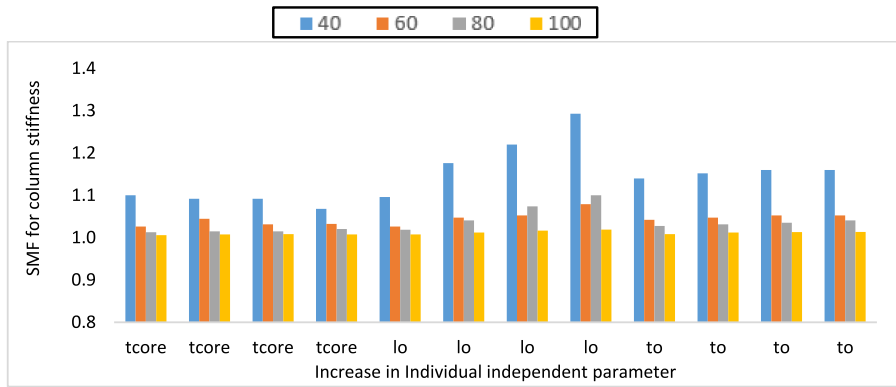
(c) Percentage increase in total concrete volume of the structure when only the column and outrigger stiffness is increased under EQ loads

Fig. 9 Percentage increase in total concrete volume of the structure for various β values when the independent parameters are varied

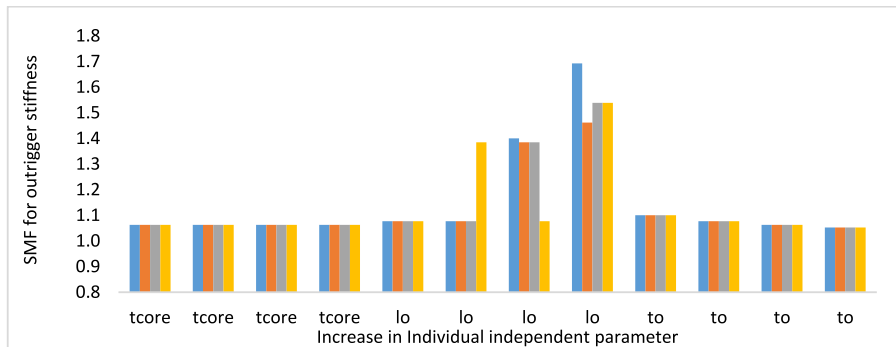
performance to be on par with the COS performance under wind loads. As mentioned earlier, increasing column and outrigger stiffness alone resulted in a lower increase in total concrete volume than compared with models with increase in slab and outrigger stiffness alone.

From Fig. 10a, it's visible that with increase in height of the storeys, the SMF for column stiffness is reducing and it

is the least for the highest storey models. It's also noticeable that SMF for column stiffness has more significant variation for models where l_o is increased. In 40 storey models with l_o 16 m on each side (building width 50 m), there is a SMF of 1.29 for axial stiffness of column and only SMF of 1.02 in 100 storey models which shows that, for higher storey models the SMF for column stiffness has reduced. When



(a) Variation in column stiffness when only the column and outrigger stiffness in the models are increased



(b) Increase in outrigger stiffness when only the column and outrigger stiffness in the models are increased

Fig. 10 SMF for column and outrigger stiffness when only the column and outrigger stiffness in the models are increased under wind loads

comparing individual storey heights, the SMF for column stiffness for variation in t_{core} and t_o is found to be nearly stagnant or not much variation is observed when compared with models where l_o is increased.

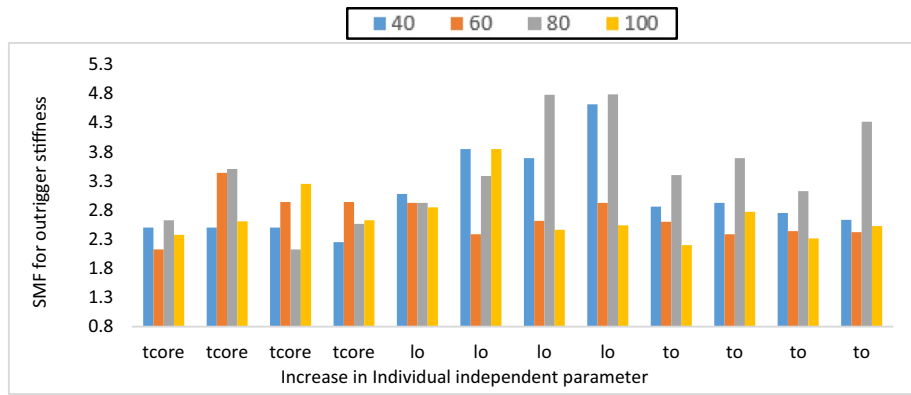
From Fig. 10b, it's visible that with increase in height of the storeys, SMF for outrigger stiffness is stagnant for variation in t_{core} and t_o . Only the column stiffness is varied accordingly to reduce the PIC_{HOS} with a moderate increase in the outrigger stiffness for getting minimum increase in total concrete volume but, in cases of l_o increase (models having 40, 45 and 50 m), significant increase in the outrigger thickness along with axial stiffness of column, led to a minimum total concrete volume increase. In 40 storey models, with l_o 16 m on each side (building width 50 m), there is a SMF of 1.69 for bending stiffness of outrigger and SMF of only 1.08 for l_o 8.5 m on each side (building width 35 m).

For 50 m models, with SMF of 1.08 for outrigger stiffness and significant increase in column stiffness, the total concrete volume is rising and so trails with a significant variation in outrigger stiffness along with column stiffness

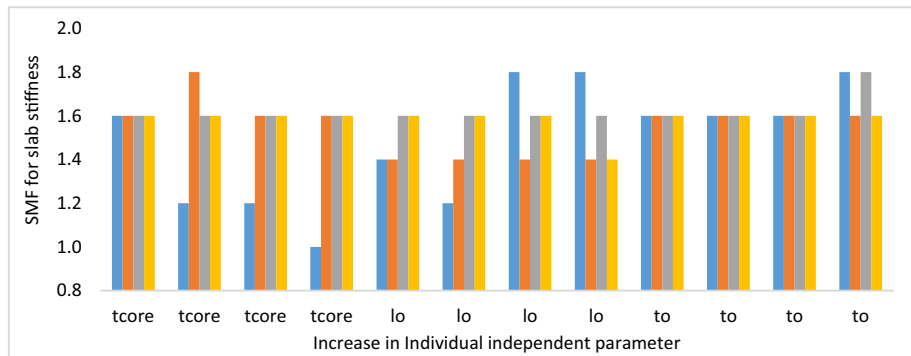
increase led to the minimum increase in total concrete volume for an effective performance of hybrid outrigger system. This significant variation in outrigger stiffness along with column stiffness increase is working only for models having larger widths but in other models having 35 m and 40 m, moderate increase in outrigger stiffness and significant increase in column stiffness led to the minimum increase in total concrete volume.

Figure 11a and b shows the SMF for stiffness of the outrigger and the slab, respectively, for the comparison study under wind loads. Results from Fig. 11a and b take into account models whose stiffness changes are made to the slab and outriggers alone to bring HOS performance in line with COS performance. Increasing stiffness of the outrigger and the slab alone led to a rise in total concrete volume when compared with models having increase in stiffness of the outrigger and the column alone.

From Fig. 11a, it's noticed that a consistent pattern is not visible in the case of increase in outrigger stiffness for variation in the height of the models or in the individual stiffness



(a) Increase in outrigger stiffness when only slab and outrigger stiffness are increased under wind loads



(b) Increase in slab stiffness when only slab and outrigger stiffness are increased under wind loads

Fig. 11 SMF for outrigger and slab stiffness when only slab and outrigger stiffness is increased under wind loads

parameter, but increase in outrigger stiffness is comparatively more for models where l_o is increased compared with models where t_{core} and t_o is varied. This inconsistent variation is due to significant rise in total concrete volume when the slab stiffness is increased. Therefore for optimizing the total concrete volume to a minimum for an effective performance of HOS, trials has been done with significant increase in outrigger stiffness and moderate increase in stiffness of slab.

The increase in outrigger stiffness alone did not effectively help in reducing the PIC_{HOS} but with increase in stiffness of the outrigger and the slab together helped in reducing the PIC_{HOS} with a minimum increase in total concrete volume. From Fig. 11b, it's visible that the SMF for stiffness of the slab did not have much effect when the height of the model is increased for variations in t_{core} and t_o except for 40-storey models. Comparatively, a decrease in slab stiffness is seen to be effective in the case of 40 storey models when t_{core} is increased, a stagnant effect when t_o be increased and rise in the slab stiffness for l_o increase. An increased slab stiffness with height is visible when l_o is incremented.

Figure 12a and b display the SMF for column and outrigger stiffness, respectively for the comparison study under EQ loads. Figure 12a shows that the SMF for column stiffness

tends to reduce as storey height increases, and it is the lowest for 100-storey models.

For getting minimal increase in total concrete volume under EQ loads, axial column and outrigger stiffness alone is incremented. It is noticed that for increased width of the model, a higher axial stiffness with a moderate increase in outrigger stiffness reduced the PIC_{HOS} comparable to PIC_{COS} , but the concrete volume drastically increased. To eliminate that drastic rise in concrete volume, trails are made to have a significant increase in the outrigger stiffness along with the column stiffness. It is seen that, for models with higher l_o or width of the building, a significant increase in outrigger and column together gives least total concrete volume increment.

For instance, in 60-storey models, with l_o 16 m on each side (building width 50 m), a SMF of 1.37 for column stiffness and a SMF of 1.08 for outrigger stiffness gives a 14% increase in total concrete volume when compared with the volume of COS base model, but a SMF of 1.11 for column stiffness and a SMF of 3.69 for outrigger stiffness gives only 7% increase in total concrete volume. Thus, for obtaining minimal increase in total concrete volume for models studying variation in l_o (models having l_o 11, 13.5 and 16 m or corresponding width of the buildings as 40 m, 45 m and

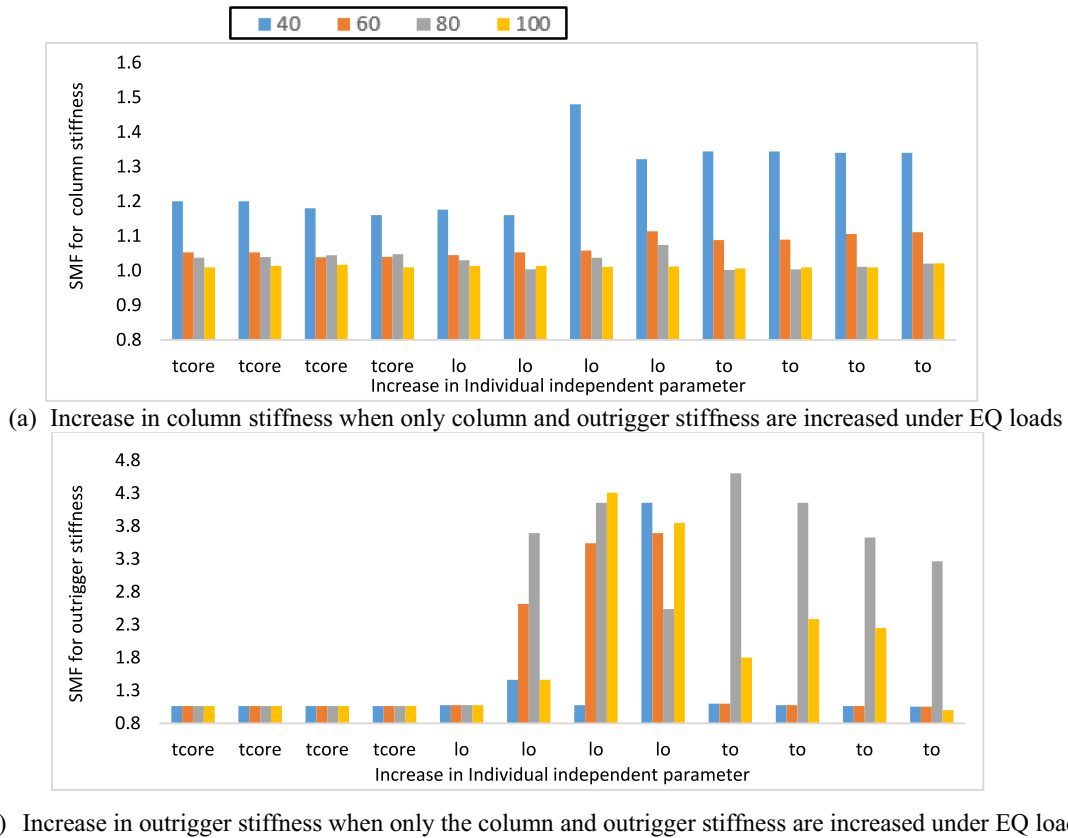


Fig. 12 SMF for column and outrigger stiffness when only the column and outrigger stiffness are increased under EQ loads

50 m) under EQ loads, drastic rise in SMF for outrigger stiffness with a significant increase in column axial stiffness is performed and this can be observed from Fig. 12a and b, l_o variation results.

This significant variation in SMF of outrigger stiffness for getting minimal increase in total concrete volume is also visible in the results of 80 and 100-storey models where t_o is varied. From Fig. 12a and b, in models where t_{core} is varied, significant increase in column stiffness and moderate increase in outrigger stiffness gave an effective performance for all the building heights considered. Thus, Figs. 9, 10, 11 and 12 briefly explains the evaluated SMF for the individual stiffness parameter and the total concrete volume increase for the HOS performance to be on par with the COS performance under both wind and EQ loads.

Conclusion

Hybrid outrigger system adopts collectively behavioural efficacy of conventional outrigger system and space efficiency of virtual outrigger system. COS shows an improved resistance to lateral deformations compared to HOS. This study

quantifies and compares the efficiency of both COS and HOS using a performance based analysis, and also portrays how the performance of HOS can be enhanced to be comparable to COS using an optimization study. The optimization study performs various trials for each β variation to improve HOS’ performance by raising the stiffness parameters, while keeping the increase in total concrete volume of the structure to a minimum. The results of the analysis lead to the subsequent conclusions.

- In the 60, 80, and 100 storey models for the EQ loads, the COS system’s optimum position is higher than the HOS, while in the 40 storey models, the HOS optimum position is higher than the COS system. In the case of wind loads, HOS has a higher optimal placement than COS for all four building heights.
- A higher PIC_{wind} and PIC_{EQ} value is found in the models with HOS compared to the COS system in their optimum position proving the improved resistance capacity of COS to lateral loads. PIC values of HOS for 40 to 100 storeys exhibits an increase of 10 to 1.1, 20.2 to 2.2 and 12.5 to 1.9% for variation in core thickness, length

of outrigger arm, and outrigger thickness, respectively, compared to PIC values of COS.

- Increase in total concrete volume under wind and EQ loads are greater for models with enhanced outrigger and slab stiffness than for models with increased column and outrigger stiffness. The increase in total concrete volume for PIC_{HOS} to be at par with PIC_{COS} under wind loads varied from 1.4 to 9, 1.15 to 3.1, 0.98 to 5.6% and 0.9 to 1.51% in 40, 60, 80 and 100 storeys, respectively in models where column and outrigger stiffness alone is increased, and from 3.2 to 13.8%, 2.7 to 3.9%, 1.6 to 5.7% and 1 to 2% in 40, 60, 80 and 100 storeys, respectively in models where slab and outrigger stiffness alone is increased. The increase in total concrete volume for the same under EQ loads varied from 3.9 to 16%, 1.6 to 3.8%, 2.2 to 5.2%, and 0.7 to 2.5% in 40, 60, 80 and 100 storeys, respectively for models where column and outrigger stiffness alone is increased.
- For PIC_{HOS} to be comparable with PIC_{COS}, increase in the total concrete volume of HOS reduces from 1.4–16.5% to 0.6–2.5% as the model's height increases from 40 to 100 storeys, respectively, suggesting that the HOS with marginal increase in total concrete volume can perform effectively for taller structures.

The study is limited to uniform material properties, cross-section and sizes for the structural elements throughout the height of the building. Study pertaining to the reduction in cross-section of the vertical elements at higher levels has to be performed to analyse the practical implementation of HOS in taller structures. Further, connection detailing of outrigger to the core and columns has to be addressed for proper implementation of HOS in taller structures.

Acknowledgements We appreciate all of the assistance from the Manipal Academy of Higher Education in Manipal, Karnataka, India.

Funding Open access funding provided by Manipal Academy of Higher Education, Manipal. The author(s) received no financial support for the research, authorship, and/or publication of this article.

Data availability statement The corresponding author will provide the datasets produced during and/or analysed during the current investigation upon reasonable request.

Declaration

Conflict of interest There are no declared competing interests of the authors that are pertinent to the subject matter of this study.

Open Access This article is licensed under a Creative Commons Attribution 4.0 International License, which permits use, sharing, adaptation, distribution and reproduction in any medium or format, as long as you give appropriate credit to the original author(s) and the source, provide a link to the Creative Commons licence, and indicate if changes were made. The images or other third party material in this article are

included in the article's Creative Commons licence, unless indicated otherwise in a credit line to the material. If material is not included in the article's Creative Commons licence and your intended use is not permitted by statutory regulation or exceeds the permitted use, you will need to obtain permission directly from the copyright holder. To view a copy of this licence, visit <http://creativecommons.org/licenses/by/4.0/>.

References

1. R.S. Nair, Eng J. **35**(4), 140–146 (1998)
2. B. S. Smith, A. Coull, A Wiley interscience publication. (Wiley, New York, 1991)
3. B.S. Smith, I. Salim, Comput. Struct. **17**(1), 45–50 (1983)
4. B. S. Taranath, Concrete reinforcing steel institute (2006)
5. A. Horton, A Virtual outriggers in tall buildings. <https://fdocuments.in/document/virtual-outriggers-in-tall-buildings.html> (2000)
6. T.S. Eom, H. Murmu, W. Yi, Int. J. Concr. Struct. Mater. **13**(1), 1–13 (2019). <https://doi.org/10.1186/s40069-018-0311-2>
7. R. Kamgar, P. Rahgozar, Asian. J. Civ. Eng. **20**(6), 759–768 (2019)
8. J. Lee, M. Bang, J.Y. Kim, Struct. Des. Tall Build. **17**(4), 839–851 (2008). <https://doi.org/10.1002/tal.406>
9. J.C.D. Hoenderkamp, Adv. Struct. Eng. **12**(3), 385–397 (2009)
10. X. Zhao, X. Jiang, IABSE Symposium Report **102**(37), 483–490 (2014)
11. M. A. Moghadam, A. Meshkat-Dini, A. R. S. M., Moghadam, Proceedings of the 7th International Conference on Seismology & Earthquake Engineering, Tehran Iran, 7, p.18–21 (2015)
12. F. Nouri, P. Ashtari, Wind Struct. Int. **20**(4), 489–508 (2015)
13. D.M. Patil, K.K. Sangle, Structures **8**, 1–16 (2016). <https://doi.org/10.1016/j.istruc.2016.07.005>
14. H. S. Park, E. Lee, S. W. Choi, B. K. Oh, T. Cho, Y. Kim, Eng. Struct. **117**, p. 496–505 (2016) <https://doi.org/10.1016/j.engstruct.2016.02.027> (2016).
15. H.S. Kim, Eng. Struct. **150**, 91–97 (2017)
16. N.E. John, K. Kamath, Asian. J. Civ. Eng. **24**, 759–778 (2022). <https://doi.org/10.1007/s42107-022-00528-7>
17. N.E. John, K. Kamath, Struct. Eng. Mech. **86–4**, 503–518 (2023). <https://doi.org/10.12989/sem.2023.86.4.503>
18. N. E. John, K. Kamath 2023 Struct. Des. Tall Build., e2080. <https://doi.org/10.1002/tal.2080>
19. K.S. Moon, Int. J. High-Rise Build. **5**(1), 13–20 (2016)
20. D. I. Samarakkody, D. P. Thambiratnam, T. H. T. Chan, P. H. N. Moragaspiya, Constr Build Mater. **143**, 659–672 (2017) <https://doi.org/10.1016/j.conbuildmat.2016.11.091>
21. Y. Chen, Z. Zhang, Struct. Des. Tall. Build. **27**(1), 1–16 (2018)
22. W. F. Baker, C. Brown, J. J. Pawlikowski, D. S. Rankin, Int. Conf. Case Hist. Geotech. Eng 2013. Available from: <http://scholarsmine.mst.edu/icchge/7icchge/session10/5%0AThis> (2013)
23. I. B. A. A. Khan, P. N. G. Gore, IOSR J. Mech. Civ. Eng. (IOSR-JMCE), **15**(6): 22–29 (2018) <https://doi.org/10.9790/1684-1506012229>
24. I. Mousleh, M. Batikha, Int. Conf. on Contemp. Issues in Sci. Eng. & Mgmt., <https://www.researchgate.net/publication/329403354> (2020)
25. IS 875: 1987 IS 875-1: Code of Practice for Design Loads (Other Than Earthquake) For Buildings and Structures, Part 1: Dead Loads. Bureau of Indian Standards. (1987)
26. IS 875: 1987 IS 875-2: Code of Practice for Design Loads (Other Than Earthquake) For Buildings and Structures, Part 2: Imposed Loads. Bureau of Indian Standards. (1987)

27. IS 875: 2015 IS 875-3: Code of Practice for Design Loads (Other Than Earthquake) For Buildings and Structures, Part 3: Wind Loads. Bureau of Indian Standards. (2015)
28. IS, Part-I-2016 Criteria for Earthquake resistant design of structures, Part 1: General Provisions and buildings. Bureau of Indian Standards, New Delhi **1893**(December), 1–27 (1893)
29. IS 16700: 2017, Criteria for Structural safety of tall concrete buildings. Bureau of Indian Standards, New Delhi, 2017, p.1–44 (2017)
30. IS 456, Concrete, Plain and Reinforced. Bureau of Indian Standards, New Delhi, pp. 1–114 (2000)
31. M. Husain, H. Hassan, H.A. Mohamed, E.S. Elgharbawy, J. Appl. Eng. Sci. **19**(3), 570–577 (2021). <https://doi.org/10.5937/jaes0-30837>
32. P.C. Lin, T. Takeuchi, R. Matsui, Eng. Struct. **194**(May), 441–457 (2019). <https://doi.org/10.1016/j.engstruct.2019.05.078>

Publisher's Note Springer Nature remains neutral with regard to jurisdictional claims in published maps and institutional affiliations.